CHEMISTRY OF MATERIALS
Communication

Chem. Mater. **2009,** *21,* 2583–2585 2583
DOI:10.1021/cm9006537

Structural Model of Rat Dentin Revisited

Shing-Jong Huang,[†] Yi-Ling Tsai,[†] Yuan-Ling Lee,[‡] Chun-Pin Lin,*[,‡] and Jerry C. C. Chan*[,†]

[†]*Department of Chemistry, National Taiwan University, No. 1, Sec. 4, Roosevelt Road, Taipei, Taiwan, and* [‡]*School of Dentistry, National Taiwan University Hospital, National Taiwan University, No. 7, Chung San South Road, Taipei, Taiwan*

Received March 7, 2009
Revised Manuscript Received April 24, 2009

The mineral phase of dentin consists mainly of apatite, which is thermodynamically the most stable phase of calcium phosphates.[1] Although solid-state NMR has been actively applied in the field of biomineralization, the studies focusing on dentin are relatively scarce compared to those on bone and enamel.[2−11] In our previous work,[12,13] we have characterized a series of dentin samples taken from Wistar rats of different ages using ^{31}P solid-state NMR spectroscopy. Three phosphorus phases, viz. hydroxyapatite (HAp), OH-deficient apatite (HDAp), and amorphous calcium phosphate (ACP), have been identified and quantified. In particular, the ACP phase contains mainly the species of HO−H···O−PO_3^{3-} and HPO_4^{2-}. Because the organic matrix of the dentin sample is not removed, the ^{31}P signal of the phosphoproteins may have minor contribution to that of ACP.[10,14] In our preliminary model, the apatite crystallites comprising HAp and HDAp are embedded in the ACP matrix.[12] As rats mature with age, there are significant changes in the water content and amount of phosphorus in the ACP phase. Because the homonuclear ^{31}P second moments determined for the HDAp are rather similar, whereas the data of ACP show a significant variation for the samples of different ages, we presumed that HDAp constitutes the core of the apatite crystallites and the HAp phase constitutes the shell. In this work, we have derived a new solid-state NMR strategy, viz. ^{31}P−^{31}P spin diffusion, to directly probe for the spatial relationship of HAp, HDAp, and ACP.

The idea of the pulse sequence shown in Figure 1a is to use the effect of ^{31}P−^{31}P spin diffusion to probe for the proximity of HAp to HDAp, and that of ACP to HDAp. After the ^{1}H−^{31}P Lee−Goldburg cross-polarization (LGCP) period,[15] the ^{31}P magnetizations of HAp and ACP are flipped onto the *z*-axis. The ^{31}P−^{31}P spin diffusion would occur during the mixing time. Because the ^{31}P chemical shifts of HAp, HDAp, and ACP are very similar (ca. 3.2 ppm) and their signal linewidths are relatively small (≤600 Hz), it is not necessary to apply ^{1}H decoupling or recoupling during the mixing time. The rotational echo double resonance[16] (REDOR) dephasing period is then used to select the ^{31}P signals that are relatively remote from ^{1}H species. Experimentally, we find that a REDOR dephasing period of 2 ms can effectively suppress the PO_4^{3-} signal of HAp or the HPO_4^{2-} signal of octacalcium phosphate (data not shown). Using the pulse sequence of Figure 1a, a series of ^{31}P{^{1}H} heteronuclear correlation (HETCOR) spectra were measured at different spin diffusion times for the dentin sample of a Wistar rat of 6-week old. Referring to Figure 2, the presence of any cross-peaks of the HETCOR spectra would indicate a relay of signal transfer from ^{1}H to the ^{31}P of HAp or ACP, and then to the ^{31}P of HDAp. Accordingly, the control spectrum of mixing time equal to 100 μs has very limited signals under the same experimental conditions (see the Supporting Information).

Figure 3 plots the signal integrals corresponding to the region of HAp and ACP as a function of the spin diffusion time, in which the two sets of data have been corrected for the residual signals at zero mixing time and then normalized individually. The HAp/HDAp data were analyzed by a simple spin diffusion model (see the Supporting Information). Similar analysis was carried out for the ACP/HDAP data. As shown in Figure 3, it is remarkable to find that the signal buildup rate is very similar for HAp/HDAP and ACP/HDAP. The time constants (τ_{SD}) of the ^{31}P spin diffusion are both approximately equal to 1 s, which is significantly shorter than the spin−lattice relaxation time of the ^{31}P signal (68 to 78 s).[12]

Figure 1b shows the pulse sequence we used to probe for the proximity of HAp to ACP, which is followed from the ^{1}H−^{31}P−^{1}H strategy documented in the literature.[17,18] The

*Corresponding authors. E-mail: pinlin@ntu.edu.tw (C.-P.L.); chanjcc@ntu.edu.twn (J.C.C.C.)

(1) LeGeros, R. Z. Calcium Phosphates in Oral Biology and Medicine; Karger: Basel, 1991; Vol. 15.
(2) Reid, D. G.; Duer, M. J.; Murray, R. C.; Wise, E. R. *Chem. Mater.* **2008**, *20*, 3549.
(3) Kaflak, A.; Kolodziejski, W. *Magn. Reson. Chem.* **2008**, *46*, 335.
(4) Best, S. M.; Duer, M. J.; Reid, D. G.; Wise, E. R.; Zou, S. *Magn. Reson. Chem.* **2008**, *46*, 323.
(5) Wise, E. R.; Maltsev, S.; Davies, M. E.; Duer, M. J.; Jaeger, C.; Loveridge, N.; Murray, R. C.; Reid, D. G. *Chem. Mater.* **2007**, *19*, 5055.
(6) Wilson, E. E.; Awonusi, A.; Morris, M. D.; Kohn, D. H.; Tecklenburg, M. M. J.; Beck, L. W. *Biophys. J.* **2006**, *90*, 3722.
(7) Kaflak, A.; Chmielewski, D.; Gorecki, A.; Slosarczyk, A.; Kolodziejski, W. *Solid State Nucl. Magn. Reson.* **2006**, *29*, 345.
(8) Jäger, C.; Groom, N. S.; Bowe, E. A.; Horner, A.; Davies, M. E.; Murray, R. C.; Duer, M. J. *Chem. Mater.* **2005**, *17*, 3059.
(9) Kolodziejski, W. In Topics in Current Chemistry; Klinowski, J., Ed.; Springer Verlag: Berlin, 2004; Vol. 246, p 235.
(10) Wu, Y.; Ackerman, J. L.; Strawich, E. S.; Rey, C.; Kim, H. M.; Glimcher, M. J. *Calcif. Tissue Int.* **2003**, *72*, 610.
(11) Wu, Y. T.; Glimcher, M. J.; Rey, C.; Ackerman, J. L. *J. Mol. Biol.* **1994**, *244*, 423.
(12) Tseng, Y. H.; Tsai, Y.-L.; Tsai, T. W. T.; Chao, J. C. H.; Lin, C.-P.; Huang, S.-H.; Mou, C. Y.; Chan, J. C. C. *Chem. Mater.* **2007**, *19*, 6088.
(13) Tseng, Y.-H.; Tsai, Y.-L.; Tsai, T. W. T.; Lin, C.-P.; Huang, S.-H.; Mou, C.-Y.; Chan, J. C. C. *Solid State Nucl. Magn. Reson.* **2007**, *31*, 55.
(14) Cho, G. Y.; Wu, Y. T.; Ackerman, J. L. *Science* **2003**, *300*, 1123.
(15) Ladizhansky, V.; Vega, S. *J. Chem. Phys.* **2000**, *112*, 7158.
(16) Gullion, T.; Schaefer, J. *J. Magn. Reson.* **1989**, *81*, 196.
(17) Duer, M. J.; Friscic, T.; Murray, R. C.; Reid, D. G.; Wise, E. R. Biophys. J. 2009, in press.
(18) Maltsev, S.; Jäger, C. *Solid State Nucl. Magn. Reson.* **2008**, *34*, 175.

Published on Web 05/12/2009

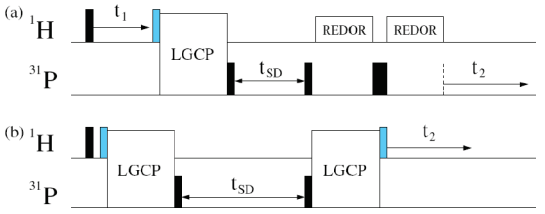

Figure 1. Pulse sequences employed to probe for the proximity of different phosphorus phases in rat dentin. During the LGCP period, the ^{1}H rf field and its offset are adjusted to fulfill the LG condition, whereas the rf field of ^{31}P is ramped through the Hartmann−Hahn matching condition. LG irradiation can suppress the ^{1}H−^{1}H spin diffusion during the CP period. The rectangles in black denote $\pi/2$ or π pulses. The grayish rectangles before the LGCP blocks denote the theta pulses that align the magnetization onto the effective spinlocking field. The one after the LGCP block flips the magnetization onto the x-axis. The period t_{SD} denotes the mixing time for ^{31}P−^{31}P spin diffusion. (a) Pulse sequence for the spectrum shown in Figure 2. (b) Pulse sequence for the spectra shown in Figure 4.

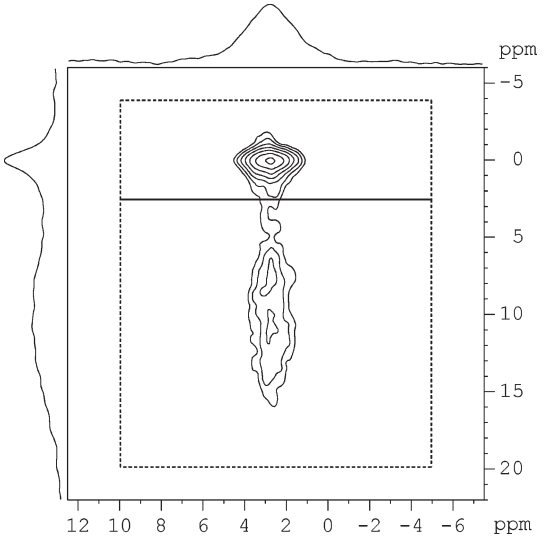

Figure 2. ^{31}P{^{1}H} HETCOR spectrum obtained by the pulse sequence of Figure 1a. The vertical and horizontal axes correspond to the ^{1}H and ^{31}P dimensions, respectively. Experimental conditions: spinning frequency 10 kHz; ^{1}H field strength 50 kHz; ^{31}P field strength 46−57 kHz; LGCP contact time 2.5 ms; mixing time 2 s; total REDOR dephasing time 2 ms; each REDOR π pulse 10 μs; number of transients 32; t_1 increments 128; t_1 step 50 μs; hypercomplex approach; recycle delay 2 s. The ^{31}P signals transferred from HAp to HDAp (HAp/HDAp) and from ACP to HDAp (ACP/HDAp) were quantified by integrating the two rectangular regions centered at the ^{1}H chemical shifts of 0.2 and 11 ppm, respectively.

first LGCP module prepares the ^{31}P signals of HAp and ACP. After the mixing period for ^{31}P−^{31}P spin diffusion, the ^{31}P signals are transferred back to ^{1}H for detection by the second LGCP module. By a judicious choice of the first LGCP contact time, the relative ^{1}H signal intensities of HAp and ACP could be made different from their equilibrium values. As the spin diffusion time increases, the relative signals of HAp and ACP will approach their equilibrium values. Figure 4 shows the HAp and ACP signals as a function of the ^{31}P−^{31}P spin diffusion times, from which their relative signal intensities were determined and analyzed in a similar fashion to that shown in Figure 3. With reference to Figure 5, the two initial conditions, in which either ACP or HAp were suppressed, consistently

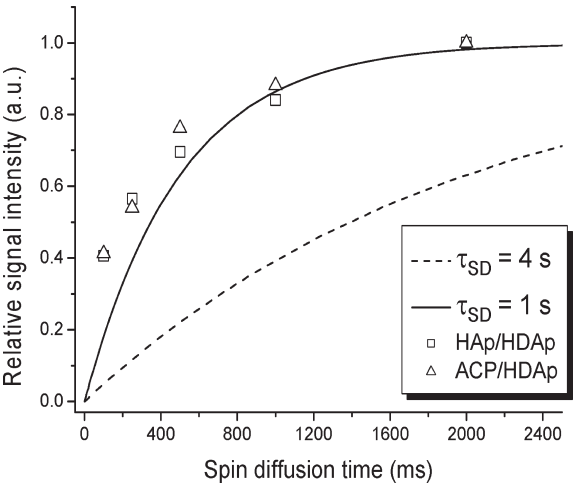

Figure 3. Plot of the signal integrals of Figure 2 versus ^{31}P−^{31}P spin diffusion time. The solid and dashed lines denote the calculated results on the basis of our spin diffusion model.

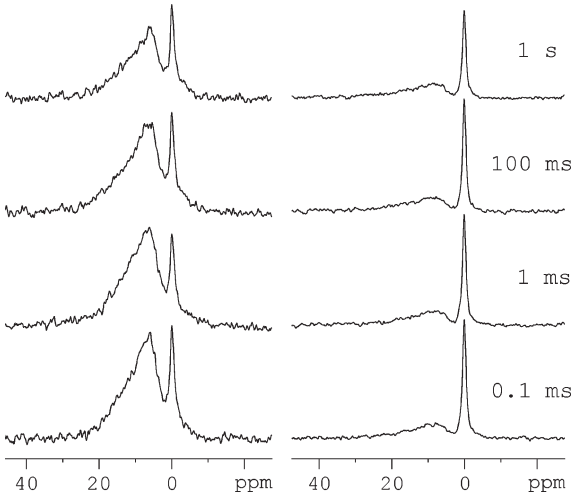

Figure 4. Selected ^{1}H spectra of different ^{31}P−^{31}P spin diffusion times obtained by the pulse sequence of Figure 1b. The first LGCP contact time was set to 0.4 (left traces) and 12 ms (right traces) to select the ACP and HAp signals, respectively. Other experimental conditions: spinning frequency 20 kHz.; second LGCP period 2 ms.

produce the same result that the spin diffusion time constant for HAp/ACP is about 6 s. These results partially justify our data analysis shown in Figure 3, in which we ignored the transfer between HAp and ACP.

Overall, the results of Figures 3 and 5 provide an unequivocal experimental evidence that the ^{31}P spin diffusion rates of HAp/HDAP and ACP/HDAp are approximately the same, whereas the rate of HAp/ACP is considerably smaller. In other words, ACP and HDAp are in close proximity, and so are HAp and HDAp. Because the phases of HAp and ACP are spatially more remote, our earlier dentin structural model should be revised in such a way that the core of the apatite crystallites is assigned to HAp, instead of HDAp. The quantification of each individual phase as described previously remains valid.[12] Figure 6 shows the revised structure of Wistar rat dentin. Note that the phase of HDAp has a wide range of levels of hydroxyl deficiency. One may attempt to deduce the

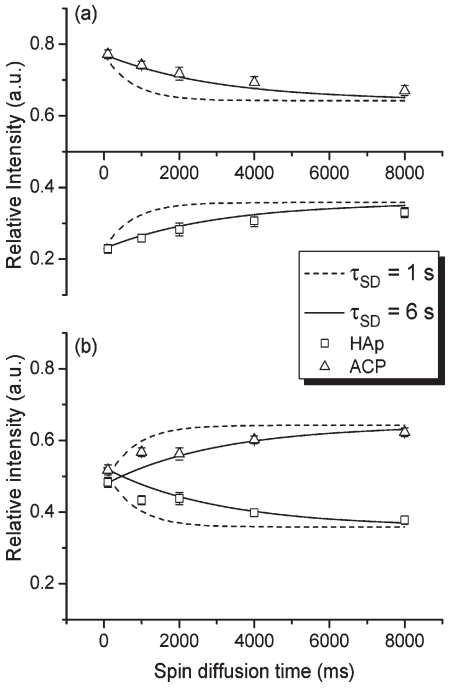

Figure 5. Plot of the ^{31}P signals of HAp and ACP as a function of the spin diffusion time. (a) Relative signals deduced from the left traces of Figure 4. (b) Relative signals deduced from right traces of Figure 4.

dimension of the apatite crystallites from the spin diffusion data. However, it is not easy to take into account the effect of $^{1}H-^{31}P$ dipole−dipole interaction, which is relatively strong in ACP, on the spin diffusion rate. In any case, the faster spin-diffusion rate for ACP/HDAp indicates that such effect would not affect our major conclusion, i.e., HAp constitutes the core of an apatite crystallite.

Dentin is a hierarchical composite material comprising type-I collagen fibrils and nanocrystalline apatite.[19] The structure of dentin has as a feature the presence of dental tubules. Therefore, dentin can be categorized further into peritubular dentin (highly mineralized) and intertubular dentin (less mineralized). A recent TEM study shows that the intertubular mineral of age-induced transparent dentin contains apatite crystallites embedded in amorphous

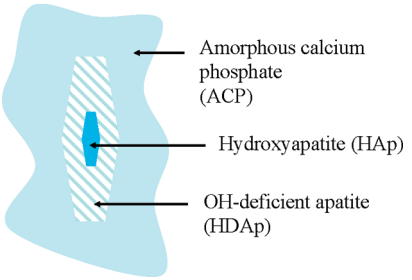

Figure 6. Revised structural model of rat dentin.

matrix.[20] Our dentin sample was prepared by grinding the rat incisors into powder form after removing the enamel layer. Therefore, the revised structural model of rat dentin shown in Figure 6 is an "average structure" of the intertubular and peritubular dentins. The most intriguing aspect of our model is that the core of each apatite crystallite consists of HAp. During the dentinogenesis, the highly phosphorylated protein, dentin phosphoprotein, would induce the precipitation of calcium phosphate in the organic matrix to trigger the mineralization of dentin at the mineralization front.[21] The mechanism of the initiation of biological mineralization has been under debate for many years.[22] The major dispute is whether a nonapatitic phase such as ACP is the nucleating phase for in vivo biological apatite, or the biomineralization process proceeds via poorly crystalline apatitic mineral. Although our NMR data cannot directly address the issue concerning the role of ACP in the incipient formation of the apatitic phase, our results are indeed consistent with the scenario that ACP provides the nucleation sites for the formation of nonstoichiometric apatite crystallites (HDAp), which may then slowly transform to HAp as driven by thermodynamics.

Acknowledgment. This work was supported by grants from the National Science Council.

Supporting Information Available: Control spectrum of the spectrally edited $^{31}P\{^{1}H\}$ HETCOR data (PDF). This material is available free of charge via the Internet at http://pubs.acs.org.

(19) Frank, R. M.; Nalbandian, J. In Teeth; Oksche, A., Vollrath, L., Eds.; Springer: Berlin, 1989; p 75.
(20) Porter, A. E.; Nalla, R. K.; Minor, A.; Jinschek, J. R.; Kisielowski, C.; Radmilovic, V.; Kinney, J. H.; Tomsia, A. P.; Ritchie, R. O. *Biomaterials* **2005**, *26*, 7650.
(21) Butler, W. T.; Ritchie, H. *Int. J. Dev. Biol.* **1995**, *39*, 169.
(22) Grynpas, M. D. *Bone* **2007**, *41*, 162.